ELSEVIER

Food Hydrocolloids 12 (1998) 29–36

FOOD HYDROCOLLOIDS

Fractal analysis of aggregates in heat-induced BSA gels

Tomoaki Hagiwara, Hitoshi Kumagai*, Kozo Nakamura

Department of Applied Biological Chemistry, Division of Agriculture and Agricultural Life Sciences, The University of Tokyo, 1-1-1 Yayoi, Bunkyo-ku, Tokyo 113, Japan

Received 19 December 1996; accepted 25 March 1997

Abstract

The fractal structure of the aggregates in heat-induced bovine serum albumin (BSA) gels was analyzed. Three kinds of BSA gels were prepared by heating BSA solutions: (i) pH 5.1 without $CaCl_2$; (ii) pH 7.0 with 30 mmol/dm^3 $CaCl_2$; and (iii) pH 7.0 with 5 mmol/dm^3 $CaCl_2$. First, from the concentration dependences of elasticity for the gels, using the theory of Shih et al. on colloidal gels, the fractal dimensions were evaluated. These BSA gels showed weak-link behavior according to the theory of Shih et al.: the limit of linearity γ_0 increased with increasing BSA concentration. Second, from the images of the aggregates in the gels obtained with confocal laser scanning microscopy, the fractal dimensions of heat-induced BSA gels were evaluated using the box counting method. The fractal dimensions D_f for the three gels evaluated from rheological measurement were close to those evaluated from image analysis, the value of D_f for the gels being ~2.6–2.8.

1. Introduction

On heating a globular protein solution, protein molecules often aggregate and gel is formed at high concentration: this phenomenon has been used in food preparation or processing. The mechanism of the aggregation has been reported to be that in which heat-denatured protein molecules stick to each other by interactions such as hydrophobic interaction and disulfide bond formation (Clark and Lee-Tuffnell, 1986). Many studies have reported that such macroscopic physical properties as elasticity of aggregate gels vary with the aggregation conditions, e.g. pH and metal ion concentrations (Egelandsdal, 1980; Richardson and Ross-Murphy, 1981; Hatta et al., 1986). However, most of the studies refer only to the correlation between the aggregation conditions and the macroscopic physical properties. The macroscopic properties of aggregate gels are considered to be closely related to the microscopic structure of the protein aggregates in the gel. Therefore, the relationship between the structure of the aggregates and the macroscopic physical properties should be investigated to systematically understand the behavior of the macroscopic physical properties of the gel.

Recently, fractal analysis has attracted attention as a quantitative analytical method that can characterize many kinds of disordered shape (Mandelbrot, 1982). A fractal is a self-similar structure which can be characterized by a non-integer dimension: the fractal dimension D_f (Mandelbrot, 1982; Vicsek, 1989). The concept of the fractal has been applied to colloid aggregation in dilute solution: some colloid aggregation experiments with techniques such as light scattering and transmission electron microscopy have shown that the aggregate structure can be characterized as a kind of fractal: the mass-fractal (Weitz et al., 1985; Schaefer et al., 1984; Weitz and Oliveria, 1984). With the fractal concept, several computer simulations have predicted numerically the structure and size distribution of aggregates in dilute solution (Meakin, 1984; Meakin et al., 1985; Brown and Ball, 1985; Family et al., 1985; Jullien et al., 1984). These predictions have been confirmed for several kinds of colloid aggregation systems (Schaefer et al., 1984; Weitz et al., 1985; Lin et al., 1990a,b; Weitz and Lin, 1986). We have already analyzed the fractal structure of the aggregates formed by heating dilute bovine serum albumin (BSA) solution with light- scattering methods (Hagiwara et al., 1996): the fractal dimension of the aggregates at pH 7.0 (apart from the isoelectric point of BSA, pH 4.9) was ~2.1, the value of which agreed with that predicted by the reaction-limited cluster–cluster aggregation model (Vicsek, 1989; Brown and Ball, 1985), while at pH 5.1 the fractal dimension was ~1.8, which agreed with that predicted by the diffusion-limited cluster–cluster aggregation model (Vicsek, 1989;Weitz and Oliveria, 1984).

The fractal structure of gels formed by aggregation has also been analyzed: Bremer et al. determined the fractal dimension of a caseinate gel prepared by addition of glucono-δ-lactone from the images obtained by confocal scanning laser microscopy (Bremer et al., 1990, 1993). In addition, they also evaluated the fractal dimension (Bremer et al., 1989, 1990, 1993) from the concentration dependence of the elastic modulus of the gel, using their theory based on

* Corresponding author.

0268-005X/98/$19.00 + 0.00.

the assumption that the strands composing the network in the gel are bent under applied stress: they showed that the value of the fractal dimension obtained from the rheological measurement agreed with that obtained from the image analysis (Bremer et al., 1990, 1993). Shih et al. (1990) evaluated the fractal dimension of boehmite alumina colloidal gels from the measurement of the elastic modulus of the gels, using a different theory. There has, however, been little research carried out on the fractal analysis of heat-induced protein gels.

In this study, from the measurements of concentration dependence of the elasticity of heat-induced BSA gels, using the theory of Shih et al. on colloidal gels, the fractal dimensions were evaluated. In addition, from the analysis of the images obtained with confocal laser scanning microscopy, the fractal dimensions of the BSA gels were calculated and the values compared with those obtained from rheological measurements.

2. Materials and methods

2.1. Theory of Shih et al.

According to the theory of Shih et al. (1990), the structure of colloidal gel (aggregate gel) is approximated as closely packed fractal flocs, and the elastic property of the gel is dominated by that of the flocs. Depending on the strength of the links between the neighboring flocs in comparison with those in the flocs, the links are classified into two types: strong and weak. In the strong-link regime, the links between the neighboring flocs have a higher elasticity than those in the flocs. For the gel with a strong link (hereafter referred to as strong-link gel), the dependence of the elasticity E and the limit of linearity γ_0 of the gels on the particle (in this study, protein) concentration ϕ can be described as follows:

$$E \sim \phi^{(3+x)/(3-D_f)} \tag{1}$$

$$\gamma_0 \sim \phi^{-(1+x)/(3-D_f)} \tag{2}$$

where D_f is the fractal dimension of the flocs ($D_f \leq 3$) and x is the backbone fractal dimension of the flocs, which varies between 1.0 and 1.3 (Shih et al., 1988). On the other hand, in the weak-link regime, the links in the flocs have a higher elasticity than those between the neighboring flocs: for the gel with a weak-link (hereafter referred to as a weak-link gel), the dependence of E and γ_0 on particle concentration ϕ can be expressed as follows:

$$E \sim \phi^{1/(3-D_f)} \tag{3}$$

$$\gamma_0 \sim \phi^{1/(3-D_f)} \tag{4}$$

2.2. Materials

Bovine serum albumin was obtained from Boehringer Mannheim GmbH (Mannheim, Germany). All other chemicals were of reagent grade.

2.3. Preparation of BSA solutions

BSA was dissolved in the three kinds of buffer: (i) 50 mmol/dm^3 acetate buffer (pH 5.1; NaCl was added to make the ionic strength of the buffer 0.1 mol/dm^3); (ii) 50 mmol/dm^3 HEPES buffer (pH 7.0; $CaCl_2$ was added to 30 mmol/dm^3); and (iii) 50 mmol/dm^3 HEPES buffer (pH 7.0; $CaCl_2$ was added a concentration of 5 mmol/dm^3). The solutions were degassed under vacuum for 3 min to remove air. The pH of the solutions was then adjusted to the pH of the buffers, using NaOH and HCl solutions.

2.4. Measurement of gel elasticity

Gels used for measuring elasticity were prepared as follows. The BSA solutions prepared above were poured into glass tubes (28 mm in outer diameter, 20 mm in inner diameter, 40 mm in height) precoated with Sigmacoat (Sigma, St Louis, MO), and each tube was closed with a Teflon cap. The samples were preheated at 50°C for 60 min to prevent the production of bubbles and then heated in a water bath at 95°C for 10 min. The heated samples were immediately cooled to 25°C in a water bath. The gels were removed from the tube and cut into a cylindrical shape (15 mm height). The cylindrical gel was stored in silicon oil at 25°C for 24 h before the measurement.

Gel elasticity was determined by a uniaxial compression test with Rheoner RE-3305 (Yamaden, Tokyo, Japan). The sample vessel used for measuring elasticity is illustrated in Fig. 1. To prevent the evaporation of the water from the gels during the measurement, the gel samples were placed in a silicon oil bath chamber equipped with a thermostatted jacket. The temperature in the oil bath chamber was set to 25°C by circulating the water in the thermostatted jacket. A cylindrical gel sample was vertically compressed with a polyacetal flat plunger of 30 mm diameter at a compression rate of 1.0 mm/s. The strain was determined as the ratio of the deformation to the initial height of the gels. The elasticity E was calculated from the linear part of the stress–strain curve over a small strain range.

2.5 Estimation of the limit of the linearity γ_0

The limit of the linearity γ_0 is difficult to determine accurately. However, only the sign of the slope of $\log\gamma_0$ versus $\log\phi$ plot is necessary for determining the value of D_f, as explained later. Therefore, γ_0 was estimated as shown in Fig. 2. In the stress–strain curve of Fig. 2, the solid line is used for elasticity evaluation. The strain value where the deviation between the ordinate value of the curve (F/S) and that of the line (E) was 5% was taken as γ_0.

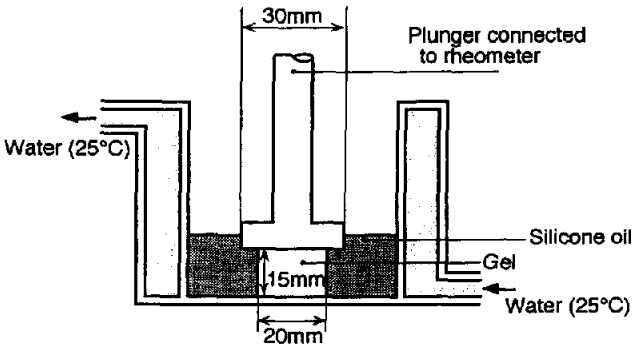

Fig. 1. Schematic diagram of the sample vessel used for the elasticity measurement of a gel.

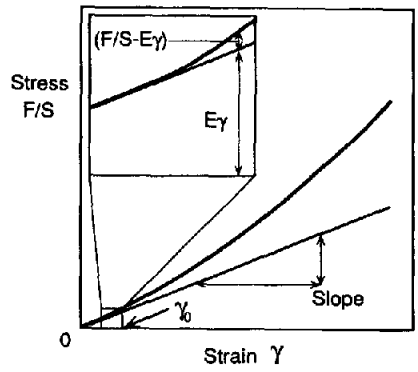

Fig. 2. Estimation of limit of linearity γ_0 from the stress–strain curve: γ_0 is γ at $|F/S - E\gamma|/E\gamma = 0.05$.

2.6. Evaluation of fractal dimension D_f from rheological data

First, γ_0 was plotted against ϕ. Because γ_0 decreases with increasing ϕ for a strong-link gel and increases with increasing ϕ for a weak-link gel (see Eqs. 2 and 4), the types of cross-links for the gel can be identified from the sign of the slope of the $\log\gamma_0$ versus $\log\phi$ plot. The fractal dimension D_f is then evaluated from the slope of the log E versus $\log\phi$ plot, using Eq. (1) for a strong-link gel and Eq. (3) for a weak-link gel.

2.7. Preparation of a gel for confocal scanning laser microscopy

The BSA solution prepared above was poured into an Eppendorf tube and preheated at 50°C in a water bath for 60 min. The preheated solution was poured into a gap of 0.18 mm between two glass plates equipped with a spacer made from Niftron tape (Nitto Denko Co., Osaka, Japan). For convenience in removing the gel from the plates and spacer, the plates were precoated with Sigmacoat and silicone grease was spread as a release agent on the surface of the spacer. The samples were heated at 95°C for 10 min. Thereafter, the sample was cooled on a stainless steel plate floated on a water bath thermostatted at 25°C. After 24 h, the gel strips were removed and cut into 5 mm squares.

The obtained gels were stained with a solution of fluorescein isothiocyanate (FITC) (Waggoner et al., 1989). For the staining solution for the gels prepared with 50 mmol/dm^3 acetate buffer, the buffer containing 0.1% w/w FITC was used. For the gels prepared with 50 mmol/dm^3 HEPES buffer containing 30 mmol/dm^3 $CaCl_2$ or 5 mmol/dm^3 $CaCl_2$, the buffer containing 0.001% w/w FITC was used as the staining solution. The gels were immersed in the staining solution for 1 h with gentle shaking. The stained gels were then mounted on a slide. Only the gels prepared with 50 mmol/dm^3 HEPES buffer were washed in fresh buffer for 1 h with gentle shaking to remove excess FITC from the gels to obtain a micrograph of good quality for image analysis, before mounting them on a slide. Cover glasses were placed around the gel as spacers, and then a cover glass was placed on top of the spacers. After the cover glasses were fixed with clear nail polish, this sample was used for confocal laser scanning microscopy observation.

2.8. The confocal laser scanning microscopy

A confocal laser scanning microscope model MRC600 (Bio-Rad Laboratories, Inc., California) was used.

2.9. Evaluation of fractal dimension D_f from the images of protein aggregates in a gel

The obtained microscopy images were digitized with the public domain NIH Image program ver.1.59 (Rasband, 1996) on the Macintosh platform. From the obtained digitized image, the fractal dimension D_f was calculated by the box counting method (Kaye, 1989); a brief procedure for the method is as follows (Bourke, 1993): a square mesh of a certain size L is laid over the object on the digitized image. The number of mesh boxes $N(L)$ that contain part of the image is counted. The fractal dimension of the protein aggregates on the image, D, is determined from the slope of the double-logarithmic plot for $N(L)$ versus L, considering the relation between the parameters:

$$N(L) \sim L^{-D} \tag{5}$$

The fractal dimension of protein aggregates of three dimensions, D_f, can be calculated from the following equation:

$$D_f = D + 1 \tag{6}$$

Computer software for fractal analysis based on the box counting method (Bourke, 1993) was used in this study.

3. Results

Fig. 3 shows stress–strain curves for the BSA gels prepared with BSA solutions of pH 5.1 (A), pH 7.0

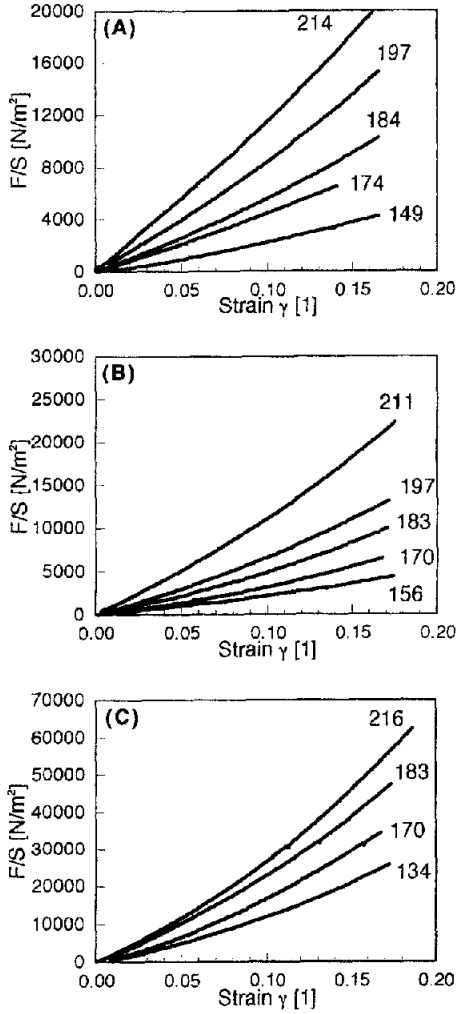

Fig. 3. Stress–strain curves for the BSA gels. Solvent: (A) 50 mmol/dm^3 acetate buffer (pH 5.1), (B) 50 mmol/dm^3 HEPES buffer (pH 7.0, containing 30 mmol/dm^3 $CaCl_2$), (C) 50 mmol/dm^3 HEPES buffer (pH 7.0, containing 5 mmol/dm^3 $CaCl_2$). The numbers in the figures represent the concentration of the gels (kg/m^3).

(containing 30 mmol/dm^3 $CaCl_2$) (B) and pH 7.0 (containing 5 mmol/dm^3 $CaCl_2$) (C).

In Fig. 4, an example of the estimation of γ_0 from a stress–strain curve is presented; the value of γ_0 was estimated to be 0.070.

Fig. 5A shows the double-logarithmic plot of γ_0 versus ϕ for the BSA gels prepared with the BSA solution of pH 5.1. Because γ_0 tended to increase with increasing ϕ, this gel is confirmed to be a weak-link gel. Fig. 5B shows the double-logarithmic plot of E versus ϕ for the same samples as those in Fig. 5A. From the slope of the plot, using Eq. (3) for weak-link gels, the fractal dimension D_f was evaluated to be 2.82. Fig. 6A,B shows the double-logarithmic plots of γ_0 versus ϕ and E versus ϕ, respectively, for BSA gels prepared with a pH 7.0 buffer (containing 30 mmol/dm^3 $CaCl_2$). From the slope of the logγ_0 versus logϕ plot (A), this gel can be confirmed to show weak-link behavior, and the fractal dimension D_f was evaluated to be 2.82 using Eq.

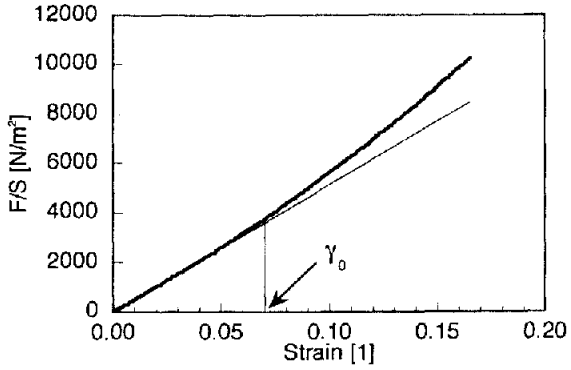

Fig. 4. An example of estimation of γ_0 from a stress–strain curve. Solvent: 50 mmol/dm^3 acetate buffer (pH 5.1). BSA concentration was 187 kg/m^3.

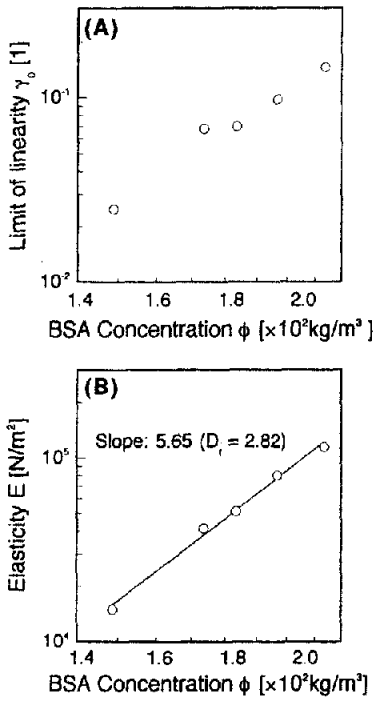

Fig. 5. The double-logarithmic plots of the limit of linearity γ_0 versus BSA concentration ϕ (A) and elasticity E versus ϕ (B). Solvent: 50 mmol/dm^3 acetate buffer (pH 5.1).

(3). Fig. 7A,B shows the double-logarithmic plots of γ_0 versus ϕ and E versus ϕ, respectively, for BSA gels prepared with a pH 7.0 buffer (containing 5 mmol/dm^3 $CaCl_2$). From the slope of logγ_0 versus logϕ, this gel is also confirmed to show weak-link behavior, and the fractal dimension D_f was evaluated to be 2.61 using Eq. (3).

A typical original image obtained with the confocal scanning laser microscopy (A) and a digitized one (B) of the gels are presented in Fig. 8. Fig. 9 shows the double-logarithmic plots of the box number $N(L)$ versus box size L for the gels prepared with the buffers of pH 5.1 (A), pH 7.0 (containing 30 mmol/dm^3 $CaCl_2$) (B) and pH 7.0

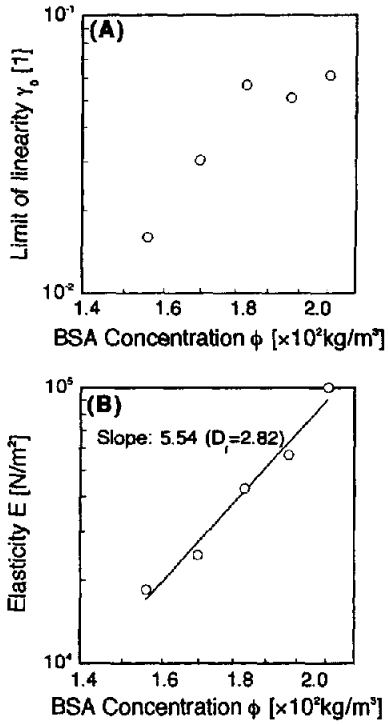

Fig. 6. The double-logarithmic plots of the limit of linearity γ_0 versus BSA concentration ϕ (A) and elasticity E versus ϕ (B). Solvent: 50 mmol/dm^3 HEPES buffer (pH 7.0, 30 mmol/dm^3 $CaCl_2$).

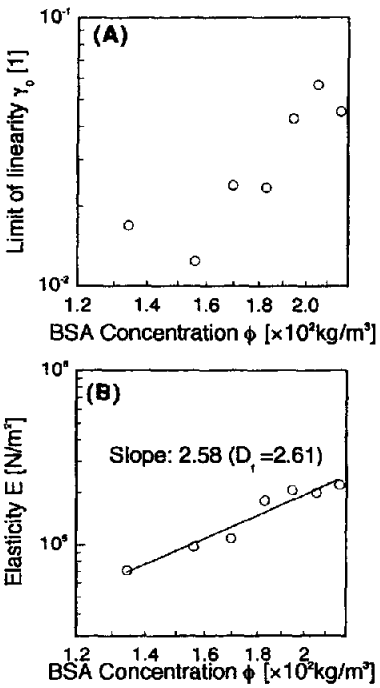

Fig. 7. The double-logarithmic plots of the limit of linearity γ_0 versus BSA concentration ϕ (A) and elasticity E versus ϕ (B). Solvent: 50 mmol/dm^3 HEPES buffer (pH 7.0, 5 mmol/dm^3 $CaCl_2$).

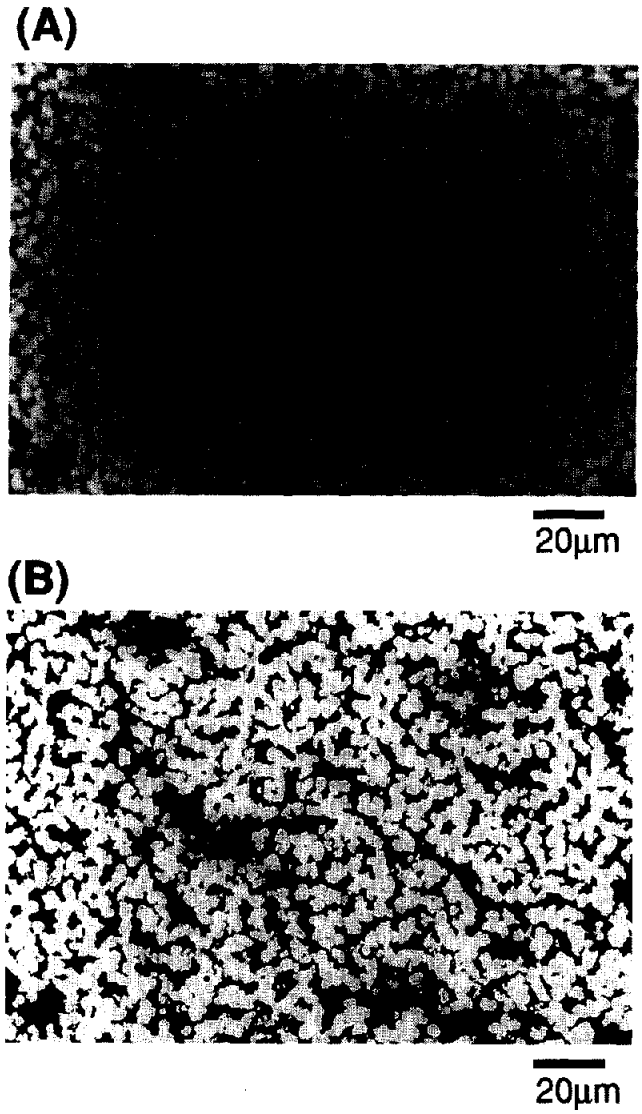

Fig. 8. Typical photograph of aggregates in the BSA gel obtained using confocal scanning laser microscopy. (A) Original image; (B) digitized image. Sample: BSA gel (concentration 174 kg/m^3) prepared with 50 mmol/dm^3 acetate buffer as a solvent.

(containing 5 mmol/dm^3 $CaCl_2$) (C). These plots show power law dependence of the box number $N(L)$ on box size L, as predicted by Eq. (5). From the slopes of the plots, the values of D of the gels were 1.81 (A), 1.81 (B) and 1.68 (C), the values of D_f being 2.81 (A), 2.81 (B) and 2.68 (C). These values of D_f were very similar to those obtained from the dependence of the elasticity of the gels on the concentration. The obtained values of D_f for these gels were larger than those of the aggregates in dilute BSA solution reported in a preceding study (Hagiwara et al., 1996). In addition, each value of D_f obtained from the image of the aggregates was almost constant, irrespective of the BSA concentration in the concentration range examined, though the data are not shown.

As shown in Figs. 5, 6, 7 and 9, the values of D_f depended on the buffers used for preparing the gel.

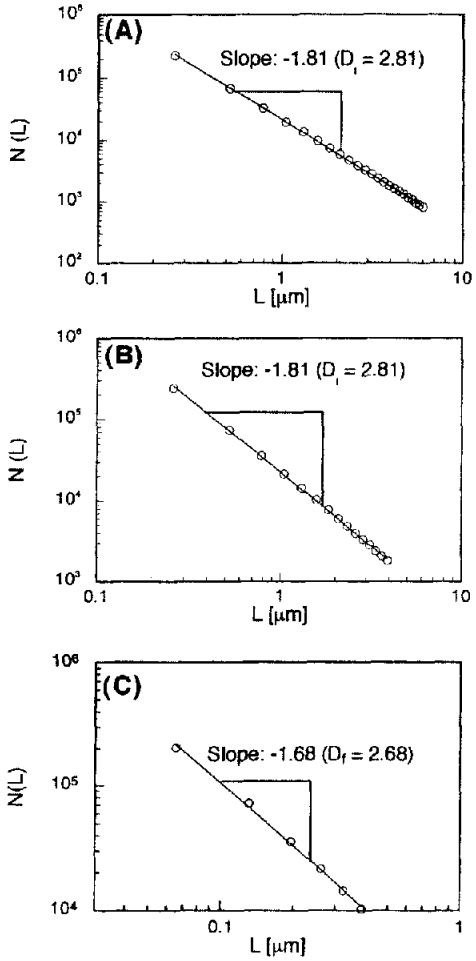

Fig. 9. Typical plots for estimation of fractal dimensions D_F. (A) 50 mmol/dm^3 acetate buffer (pH 5.1; BSA concentration 184 kg/m^3), (B) 50 mmol/dm^3 HEPES buffer (pH 7.0, 30 mmol/dm^3 $CaCl_2$; BSA concentration 197 kg/m^3), (C) 50 mmol/dm^3 HEPES buffer (pH 7.0, 5 mmol/dm^3 $CaCl_2$; BSA concentration 216 kg/m^3).

4. Discussion

Bremer et al. proposed a theory for evaluating the fractal dimension from the concentration dependence of the elasticity of aggregate gels (Bremer et al., 1989, 1990, 1993) and applied the theory to caseinate gels prepared by addition of glucono-δ-lactone (Bremer et al., 1989, 1990, 1993). In their theory, they classified gels into two types. For a type 1 gel, the strands composing the network in the gel are stretched or shrunk under applied stress, while the strands of the type 2 gels are bent under applied stress. Equations for evaluating the fractal dimensions are different between the two types of gel. It is, however, difficult to identify experimentally such strand properties and therefore to determine which equation in their theory should be used. Consequently, from the theory of Bremer et al., one can only guess the type (1 or 2) of a gel by comparing the value of the fractal dimension obtained with that evaluated by another method such as image analysis. On the other hand, the cross-link type in the theory of Shih et al. is identified in principle from the dependence of γ_0 on ϕ, as explained before. Thus, the fractal dimension D_f can be determined from rheological measurement only, the theory of Shih et al. used in this study having an advantage over that of Bremer et al.

Using the theory of Shih et al., Vreeker et al. evaluated the fractal dimensions of glycerol tristearate gel (Vreeker et al., 1992a) and whey protein gel (Vreeker et al., 1992b) from the concentration dependences of the elasticity for the gels. They used Eq. (1) (strong link) for calculating the fractal dimension. However, they did not measure the dependence of γ_0 on ϕ for the gels: they stated that the two gels belonged to the strong-link type, because the value of D_f for the gels obtained from rheological measurements agreed with those for dilute solutions evaluated from light-scattering measurements. In a preceding study (Hagiwara et al., 1996) we performed a fractal analysis of the aggregates formed by heating dilute BSA solution under the same aggregation conditions [solvent: 50 mmol/dm^3 acetate buffer (pH 5.1, NaCl was added to make the ionic strength of the buffer 0.1 mol/dm^3); heating temperature: 95°C] as those in this study, using light-scattering methods: the obtained fractal dimension was 1.8, the value of which was different from the ~2.8 evaluated in this study (Figs 5B and 9A). Kolb et al. (1985) suggested that, at a particle concentration high enough to form a gel, the fractal dimension of the aggregates could be larger than that of the aggregates formed in dilute solution, due to effects such as the interpenetration between the aggregates. From these aspects, the fractal dimension of the aggregates formed in dilute solution could disagree with that of the aggregates formed in such a concentrated solution that eventually caused gels. Therefore, it would be inappropriate to determine the cross-link type using information for a dilute solution. In this study, the cross-link type in the gel was identified from information on the gel, as shown in Figs. 5A, 6A and 7A.

As shown in Fig. 3, the apparent elasticities ($F/S/\gamma$ in Fig. 2) at a strain above γ_0 are larger than those at a strain below γ_0. The exact mechanism of such nonlinear behavior of the elasticity is unknown; however, tracing the derivation of the theory of Shih et al., it can be shown that Eqs. (1–4) in this study are derivable without supposing the specific mechanism for causing nonlinearity of the elasticity, such as bond breaking. Therefore, the equations are also applicable for the case in this study that the apparent gel elasticities at strains above γ_0 are larger than those at strains below γ_0.

Strictly speaking, the slope of the logγ_0 versus logϕ plot agrees with that of the log$E$ versus logϕ plot, according to Eqs. (3) and (4) for weak-link gels. From the plots of Figs. 5A, 6A and 7A, the apparent values of the slopes of the logγ_0 versus log ϕ plots were calculated to be 4.70 (a: pH 5.1), 4.31 (b: pH 7.0, 30 mmol/dm^3 $CaCl_2$) and 2.90 (c: pH 7.0, 5 mmol/dm^3 $CaCl_2$): these values seems to be slightly different from those of the log E versus logϕ plots. In this study, a limit of linearity γ_0 (the strain value where

the deviation between the ordinate value of the stress–strain curve and that of the line used for the elasticity evaluation) of 5% was used, as shown in Fig. 2, probably causing the error in the γ_0 values. However, the cross-link type can be discriminated by the sign of the slope of the $\log\gamma_0$ versus $\log\phi$ plot: this information is satisfactory for evaluating the fractal dimension D_f (the purpose of this study). To discuss the absolute value of the exponent in Eq. (4), it is necessary to determine γ_0 accurately by a method different from that used in this study.

The fractal dimension of protein aggregate gels can also be measured by small angle neutron scattering (Renard et al., 1996a,b). However, according to Renard et al. (1995), such fractal dimensions of β-lactoglobulin gels were different from those evaluated by rheological measurements using the theories of Bremer et al. and Shih et al. On the other hand, the fractal dimensions obtained from the confocal laser scanning microscopy were close to those obtained from rheological measurements in this study. The observation range for the small angle neutron scattering is tens to hundreds of nanometers. As shown in Fig. 9, the analysis range in the system of this study was ~0.1–5 μm. Such a fractal structure of aggregates (>0.1 μm) might reflect the behavior of gel elasticity.

Shih et al. (1990) reported that boehmite alumina colloidal gels showed strong-link behavior. No study has shown weak-link behavior from the dependence of the limit of linearity for gels on gel concentration. In this study, we found weak-link gels.

The fractal dimensions of the BSA gels prepared in this study were 2.6–2.8, depending on the buffers used for preparing the gel, as shown in Figs. 5, 6, 7 and 9. Bremer et al. reported that the fractal dimension of the caseinate gels induced by addition of glucono-δ-lactone was 2.35 from the confocal laser scanning microscopy of the gels (Bremer et al., 1990, 1993). For silica aerogels, Vacher et al. (1988) obtained a fractal dimension of 2.4 from small angle neuron scattering of the gels. It has been reported that the microstructure of gels formed by heating BSA solutions varies with the conditions of gelation, such as the pH and salt concentration of the solvent (Clark and Tuffnell, 1980; Clark et al., 1981). Therefore, the gels prepared under conditions different from those in this study may have a different fractal dimension from our findings. A further study should be done to perform the fractal analysis of various protein gels or gels formed under various gelling conditions, using the method of this study.

5. Conclusions

In this study, the fractal dimensions of heat-induced BSA gels were evaluated by two methods: the analysis of the concentration dependence of the elasticity using the theory of Shih et al. (1990) and the image analysis of the aggregate of the gels with confocal laser scanning microscopy.

The BSA gels prepared in this study showed the behavior of the weak link in the theory of Shih et al. The fractal dimensions D_f for the three gels evaluated from rheological measurement were close to those evaluated from image analysis. The values of D_f for the gels prepared in this study were 2.6–2.8. These values were larger than that of the aggregates in dilute BSA solution, suggesting that the fractal dimension of the aggregates in the gel was larger than that of the aggregates formed in dilute solution due to effects such as the interpenetration between the aggregates.

Acknowledgements

We express our thanks to Associate Professor M. Yoshida, Department of Applied Biotechnology, Faculty of Agri- culture and Agricultural Life Sciences, University of Tokyo, for his advice on confocal laser scanning microscopy. Part of this work was financially supported by a Grant-in-Aid for Scientific Research from the Ministry of Education, Science, and Culture of Japan.

References

Bourke, P. (1993). *Fractal dimension calculator user manual version 1. 5.* Auckland: Auckland University.

Bremer, L. G. B., van Vliet, T., & Walstra, P. (1989). *J. Chem. Soc. Faraday Trans. 1, 85*, 3359–3372.

Bremer, L. G. B., Bijsterbosch, B. H., Schrijvers, R., van Vliet, T., & Walstra, P. (1990). *Colloids Surfaces, 51*, 159–170.

Bremer, L. G. B., Bijsterbosch, B. H., Walstra, P., & van Vliet, T. (1993). *Adv. Colloid Interface Sci., 46*, 117–128.

Brown, W. D., & Ball, R. C. (1985). *J. Phys. A: Math. Gen., 18*, L517-L521.

Clark, A. H., & Lee-Tuffnell, C. D. (1986). In J. R. Mitchell & D. A. Ledward (Eds.), *Functional properties of food macromolecules* (pp. 203–272). London: Elsevier Applied Science.

Clark, A. H., & Tuffnell, C. D. (1980). *Int. J. Peptide Protein Res., 16*, 339–351.

Clark, A. H., Judge, F. J., Richards, J. B., Stubbs, J. M., & Suggett, A. (1981). *Int. J. Peptide Protein Res., 17*, 380–392.

Egelandsdal, B. (1980). *J. Food Sci., 45*, 570–573, 581.

Family, F., Meakin, P., & Vicsek, T. (1985). *J. Chem. Phys., 83*, 4144–4150.

Hagiwara, T., Kumagai, H., & Nakamura, K. (1996). *Biosci. Biotech. Biochem., 60*, 1757–1763.

Hatta, H., Kitabatake, N., & Doi, E. (1986). *Agric. Biol. Chem., 50*, 2083–2089.

Jullien, R., Kolb, M., & Botet, R. (1984). *J. Phys. Lett. France, 45*, 211–216.

Kaye, B. H. (1989). In D. Avnir (Ed.), *The fractal approach to heterogeneous chemistry* (pp. 55–66). Chichester: John Wiley & Sons.

Kolb, M., Jullien, R. & Botet, R. (1985). In R. Pynn & A. Skjeltrop, (Eds.), *Scaling phenomena in disordered systems* (p. 71). New York: Plenum Press.

Lin, M. Y., Lindsay, H. M., Weitz, D. A., Ball, R. C., Klein, R., & Meakin, P. (1990a). *Phys. Rev. A, 41*, 2005–2020.

Lin, M. Y., Lindsay, H. M., Weitz, D. A., Klein, R., Ball, R. C., & Meakin, P. (1990b). *J. Phys.: Condens. Matter, 2*, 3093–3113.

Mandelbrot, B. B. (1982). *The fractal geometry of nature.* San Francisco, CA: Freeman.

Meakin, P. (1984). *J. Colloid Interface Sci., 102*, 491–504.

Meakin, P., Vicsek, T., & Family, F. (1985). *Phys. Rev. B, 31*, 564–569.
Rasband, W. (1996). *NIH image manual*. Bethesda, MD: National Institutes of Health.
Renard, D., Axelos, M. A. V., & Lefebvre (1995). In Dickinson, E. & Lorient, D. (Eds.), *Food macromolecules and colloids* (pp. 390–399). Cambridge: The Royal Society of Chemistry.
Renard, D., Axelos, M. A. V., Boue, F., & Lefebvre, J. (1996a). *J. Chim. Phys., 93*, 998–1015.
Renard, D., Axelos, M. A. V., Boué, F., & Lefebvre, J. (1996b). *Biopolymers, 39*, 149–159.
Richardson, R. K., & Ross-Murphy, S. B. (1981). *Br. Polymer. J., 13*, 11–16.
Schaefer, D. A., Martin, J. E., Wiltzius, P., & Cannell, D. S. (1984). *Phys. Rev. Lett., 52*, 2371–2374.
Shih, W.-H., Shih, W. Y., & Aksay, I. A. (1988). In D. A. Weitz, L. M. Sander & B. B. Mandelbrot (Eds.), *Fractal aspect of materials: disordered systems* (p. 239). Pittsburgh, PA: Materials Research Society.
Shih, W.-H., Shih, W. Y., Kim, S.-I., Liu, J., & Aksay, I. A. (1990). *Phys. Rev. A, 42*, 4772–4779.
Vacher, R., Woignier, T., Pelous, J., & Courtens, E. (1988). *Phys. Rev. B, 37*, 6500–6503.
Vicsek, T. (1989). *Fractal growth phenomena*. Singapore: World Scientific.
Vreeker, R., Hoekstra, L. L., den Boer, D. C., & Agterof, W. G. M. (1992a). *Colloids Surfaces, 65*, 185–189.
Vreeker, R., Hoekstra, L. L., den Boer, D. C., & Agterof, W. G. M. (1992b). *Food Hydrocoll., 6*, 423–435.
Waggoner, A., de Biasio, R., Conrad, P., Bright, G. R., Ernst, L., Ryan, K., Nederlof, M., & Taylor, D. (1989). *Methods Cell Biol., 30B*, 449–478.
Weitz, D. A., & Lin, M. Y. (1986). *Phys. Rev. Lett., 57*, 2037–2040.
Weitz, D. A., & Oliveria, M. (1984). *Phys. Rev. Lett., 52*, 1433–1436.
Weitz, D. A., Huang, J. S., Lin, M. Y., & Sung, J. (1985). *Phys. Rev. Lett., 54*, 1416–1419.